ELSEVIER

Catalysis Today 38 (1997) 115–128

CATALYSIS TODAY

Forced concentration oscillations of CO and O_2 in CO oxidation over Cu/Al_2O_3

F.J.R. van Neer*, B. van der Linden, A. Bliek

Department of Chemical Engineering, University of Amsterdam, Nieuwe Achtergracht 166, 1018 WV Amsterdam, Netherlands

Abstract

The kinetics of CO oxidation over an alumina supported Cu catalyst are examined using successive oxidation and reduction cycles. Experiments were done at a temperature of 493 K with isotopically labelled gases in a tubular reactor. Surface species were monitored during transients in an FTIR flow cell. For the reoxidation of the catalyst a three-step mechanistic model is proposed. The kinetic constants are determined by mathematical modelling. The role of carbonates is found to be minor in the production of CO_2 in contrast to carbonyls which are shown to be the intermediates. A net dissociation of the CO bond was observed during reduction caused by adsorption of CO_2 on a partly reduced catalyst under formation of carboxylates and its subsequent decomposition to CO, thereby leaving oxygen on the catalyst. A complete mechanistic scheme is presented which allows us to describe qualitatively and in part quantitatively the experimental results. This study shows that the use of forced oscillations is a powerful tool with strong elucidating abilities in mechanistic investigations in heterogeneous catalysis.

Keywords: Forced oscillations; CO oxidation; Copper; Kinetics

1. Introduction

It has been demonstrated that periodic operation of catalytic reactors is very useful in many applications. Besides interesting improvement of reaction rates, selectivity or both, shown for, e.g., N_2O reduction by CO over Pt catalysts [1] and methanol synthesis over industrial catalysts [2], also simultaneous suppression of oscillations and rate enhancement in CO oxidation over Rh has been observed under imposed concentration oscillations [3]. More recently interest has risen towards the use of forced oscillations as a way to gain insight into reaction mechanisms, as an extension to step-response and steady state experiments. Renken and Thullie [4] showed that experiments with forced oscillations may be superior in discriminating between various mechanistic models. Experiments were done using imposed oscillations in CO_2 methanation with the aid of diffuse reflectance IR spectroscopy [5]. It was shown that insight can be gained on the reactive species by concentration cycling and a sequence of active intermediates was proposed and incorporated in a kinetic model. Sadhankar and Lynch [6] described the transient behaviour during NO and CO oscillations on Pt by a model which was able to predict the start-up and the long term cycle-invariant mode of this catalytic reaction in a recycle reactor. An indication for the immense difference between short and long term response can be found in the existence of multiple steady states [6]. Presently we mainly focus on the

*Corresponding author. e-mail: neer@chemeng.chem.uva.nl

PII S0920-5861(97)00045-X

information which can be extracted from the initial response to forced oscillations for CO oxidation over alumina supported Cu. No multiple steady states or self-oscillations are reported for this reaction.

Many kinetic studies of CO oxidation have been conducted using single crystals, supported Cu and supported or unsupported CuO. For single crystals a Langmuir–Hinshelwood mechanism was proposed [7] and retardation of the reaction was observed under high oxygen coverages. Crew and Madix [8] showed that on Cu(1 1 0) ordered Cu–O–Cu chains are formed in oxygen. On top of these chains a dynamic oxygen layer is observed and reaction with CO occurs at defects in this layer. The reaction initiates at the edges or kinks and subsequently more active sites become accessible and reaction proceeds. Reaction of Cu–O–Cu with CO apparently takes place at so-called chain scissions.

CO oxidation on alumina supported metallic Cu was extensively investigated by Choi and Vannice [9] using in situ IR spectroscopy before and during reaction. An Eley–Rideal mechanism was ruled out and strong evidence was obtained for reaction of adsorbed CO molecules and O atoms. Interestingly these authors suggested non-competitive adsorption and propose a model in which Cu_2O formed acts as a vacant site allowing CO adsorption where O_2 interacts with metallic Cu atoms. The reaction was found to be close to first-order in CO and zero-order in O_2 at 400 K. Szanyi and Goodman [10] showed that at 458 K significant amounts of oxygen migrate into bulk Cu during reaction even under highly reducing conditions. In TPD experiments of the latter authors subsurface oxygen diffuses to the surface and carbonates formed during reaction are removed. The latter work illustrates the possible role of subsurface oxygen and carbonates in CO oxidation.

Reaction on supported and unsupported CuO gave similar reaction orders in CO as compared to metallic Cu. For instance Yao [11] found an order in CO between 0.7 and 1.0 and no dependence of the reaction rate on the oxygen concentration for T=423–773 K. CO_2 desorption was observed to be very fast, limiting CO oxidation only below 423 K. Prokopowicz et al. [12] suggested an Eley–Rideal mechanism on the basis of a transient FTIR study at 523 K by following adsorbed CO on Cu^+, although a mechanism with adsorbed CO species could not be excluded.

In general, mechanisms proposed for catalytic oxidation reactions on metal oxides are based either on the so-called stepwise or the concerted mechanism [13,14]. The former is likely to occur at relatively high temperatures and is based on alternating oxidation and reduction of the catalyst surface: Mars and Van Krevelen mechanism. At lower temperatures (T<573 K) simultaneous oxidation of the catalyst and formation of reaction products is observed and carbonates are assumed to be an intermediate in the reaction. More recently a mechanistic study was conducted using transient methods. Dekker et al. [15,24] proposed a kinetic model for the reduction of alumina supported CuO based on step-response experiments at 453–553 K. Introducing CO over an oxidised catalyst gave at first CO_2 produced via an Eley–Rideal mechanism thereby freeing sites for CO to adsorb. Subsequently adsorbed CO reacts with in-plane oxygen atoms by Langmuir–Hinshelwood kinetics. Furthermore replenishment of oxygen by diffusion from the bulk was observed and incorporated in the model.

In the present work we try to find out whether the model proposed in Ref. [15] also adequately describes the response during the reduction part of the imposed CO/CO_2 oscillations. We monitored the role of carbonates and carbonyls under reaction conditions using transient in situ FTIR, because literature is not always unequivocal about the relevance of carbonyls or carbonates as reaction intermediates. Even more interesting is the elucidation of the mechanism of oxidation since only little work is done up to now on this reaction. To this end concentration cycling experiments with labelled and unlabelled gases were carried out. Finally the complete mechanism of CO oxidation on alumina supported CuO including reduction and oxidation of the catalyst will be tracked, thereby illustrating the merits of periodic operation in mechanistic studies.

2. Experimental

2.1. Materials

2.1.1. Gases and catalyst

All unlabelled gases were of HP or UHP grade (UCAR and Air Liquide) and purified before use (O_2 and/or H_2O removal). Gas mixtures, including the

$^{18}O_2$ mixture (Thamer Diagnostica, 96%), were made in a separate gas mixing system and stored in 0.5 or 5 l lecture bottles.

The response towards oscillations was investigated over a 10 wt% Cu/Al_2O_3 catalyst (d_p=0.105–0.140 mm). The catalyst was prepared by pore volume impregnation of γ-alumina (Ketjen CK300/000-1.5E) with an aqueous solution of $CuNO_3$ (Merck). A full description of the catalyst preparation is given elsewhere [16]. ICP-AES measurements performed on the catalyst gave a Cu content of 9.8 wt% and no significant contaminations by any other metal elements were observed.

2.1.2. *Apparatus*

Forced oscillation experiments were conducted in a tubular reactor (d_i=5.0 mm) connected to a mass spectrometer (Balzers, QMG 240) via a capillary. Gas flows were controlled by mass-flow controllers and concentration programming was carried out using a 4-way valve (Valco) with a digital valve interface controlled by a computer. The pressure in the system was 1.1 bar and was held invariant by back-pressure controllers. 50 mg of catalyst, mixed with 135 mg SiC to avoid axial dispersion and non-isothermal operation, was placed in the tubular reactor between two plugs of quartz wool. A more detailed description of this equipment can be found elsewhere [17].

In situ FTIR experiments were performed in a second experimental set-up. Main differences with the former equipment are the reactor and the state of the catalyst. The reactor for IR experiments is a flow cell with a volume of 3.6 ml, shown in Fig. 1. 40 mg of the catalyst was pressed in a ring using a pressing assembly similar to the one presented by Miura and Gonzalez [18]. The pellet was subsequently placed in the cell and fixed near the outlet thereby using a pretreated silicone ring to avoid bypassing. Under operating conditions the mixing in the IR reactor closely approximated that of an ideal CSTR because the volume of the inlet chamber (Fig. 1; V_1) is much larger than the volume of the outlet chamber (V_2). More characteristics of this cell will be published elsewhere [19].

The reaction intermediates present during the reaction on the catalyst were followed with a BIORAD FTS45A IR spectrometer and gas phase composition was analysed by a mass spectrometer (Leybold Q200). The obtained spectra were processed with WIN-IR a BIORAD software program and could be quantitatively interpreted because a linear concentration dependent MCT detector was used. This results in a linear relation between integrated absorption bands and concentrations in the gas phase or on the catalyst.

2.2. *Experimental procedures*

All experiments were performed at a temperature of 493 K, a pressure of 1.1 bar and with a total flow rate of 30 ml/min (STP). First the samples were subjected to an in situ pretreatment in which in an oxygen flow the catalyst was calcined for 1 h at 423 K whereupon at 773 K it was fully oxidised (1 h). After cooling to 493 K a stepwise increase in CO concentration in He was performed for 6 min. (0→5% CO). Subsequently the catalyst was again oxidised at 773 K and cooled to 493 K. Helium was fed to the reactor for 15 min to remove all the O_2. Only with this procedure repro-

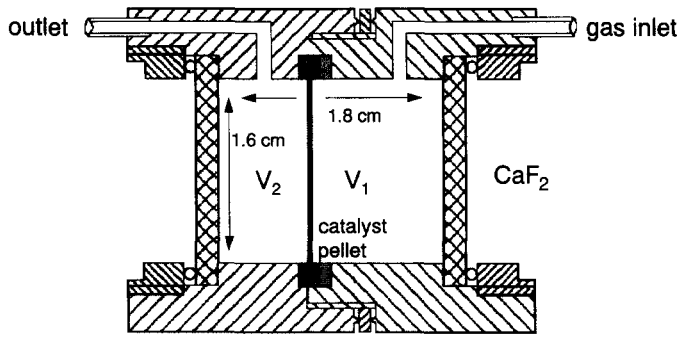

Fig. 1. FTIR flow cell. The catalyst pellet is permeable for gases. V_1=3.0 ml, V_2=0.6 ml.

ducible results could be obtained. The reduction in this pretreatment can be understood as an activation of the catalyst: by the slight reduction well defined copper particles are formed at the surface of the catalyst which remain present after reoxidation [20]. This may also lead to a higher activity [21].

Pretreatment in the IR experiments was done ex situ because the IR cell could only be used at temperatures below 573 K. After calcination, oxidation, reduction and reoxidation the catalyst pellet was transferred to the cell and heated in oxygen to 493 K where it was kept at this temperature under oxygen for at least 1 h. Hereafter, helium was passed through the cell for 15 min. No changes in time were observed in the IR spectra after this period.

Subsequently the fully oxidised Cu catalyst was subjected to various steps as depicted schematically in Fig. 3 by the thin dotted lines. We can distinguish three types of experiments:

I. subsequent reduction/oxidation cycles in a fixed bed reactor using 5% CO and 4% O_2;

II. subsequent reduction/oxidation cycles in a fixed bed reactor using 5% CO and 6.1% $^{18}O_2$;

III. subsequent reduction/oxidation cycles in the IR cell using 5% CO and 4% O_2.

Type I experiments were performed at various oscillation periods while type II experiments were carried out at a period of 100–240 s and type III at 240 s. Helium was used in all experiments to make-up the total feed flow to the reactor or the cell. The total flow was kept constant during a cycle.

3. Results and discussion

3.1. Forced oscillations of CO and O_2 (Type I)

After oxidation of the catalyst TPR results show that predominantly CuO is present on the surface. The fully oxidised catalyst was subjected to 5% CO in helium and subsequently 4% O_2 was fed to the reactor. First we focus on the response as it appears after a cycle invariant state is reached. Fig. 2 shows the time average concentration of CO_2 at the outlet when cycle invariance is reached for various frequencies. A monotonically increasing CO_2 production is observed when going from the quasi steady state at low frequencies to the relaxed steady state at the high frequency limit.

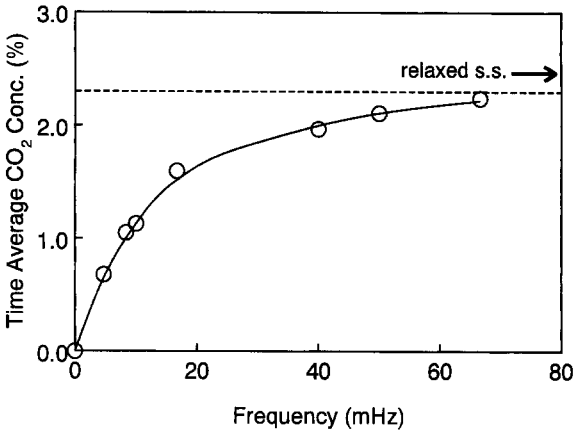

Fig. 2. Time averaged CO_2 outlet concentration at various cycle frequencies in the cycle invariant mode.

Resonance phenomena or rate enhancement above the optimal steady state are not observed, so mechanistic information cannot be obtained from these time averaged data as easily as for more simple catalytic systems [22]. However a better insight in the reaction is gained from concentration profiles in time.

In Fig. 3 the dynamic behaviour of CO_2, CO and O_2 is shown for periods of 120 s and 240 s. The same behaviour as in the step-response experiments [15] is observed after the onset of the first reduction cycle, since the same initial conditions were used. For both cycle periods a steep increase in CO_2 production right after the switch is seen. This results from the reduction of weakly bound oxygen on top of the catalyst, so-called overlayer oxygen, by CO from the gas phase via an Eley–Rideal mechanism. Subsequently the surface is occupied by CO which adsorbs easily at Cu^+ sites after removal of overlayer oxygen as demonstrated in Section 3.3. A second reduction step starts and accelerates because adsorbed CO can react with more strongly bound oxygen by a LH mechanism thereby creating additional free sites for CO to adsorb. A second maximum in the CO_2 production is obtained. This second form of adsorbed, in-plane, oxygen is assumed to be located at the same level as the Cu surface atoms, see, e.g., Ref. [8], establishing a relatively high coordination number for Cu. For a period of 240 s also a third reduction stage involving lattice oxygen can be observed. Just before the start of the oxidation cycle a significant amount of CO_2 is pro-

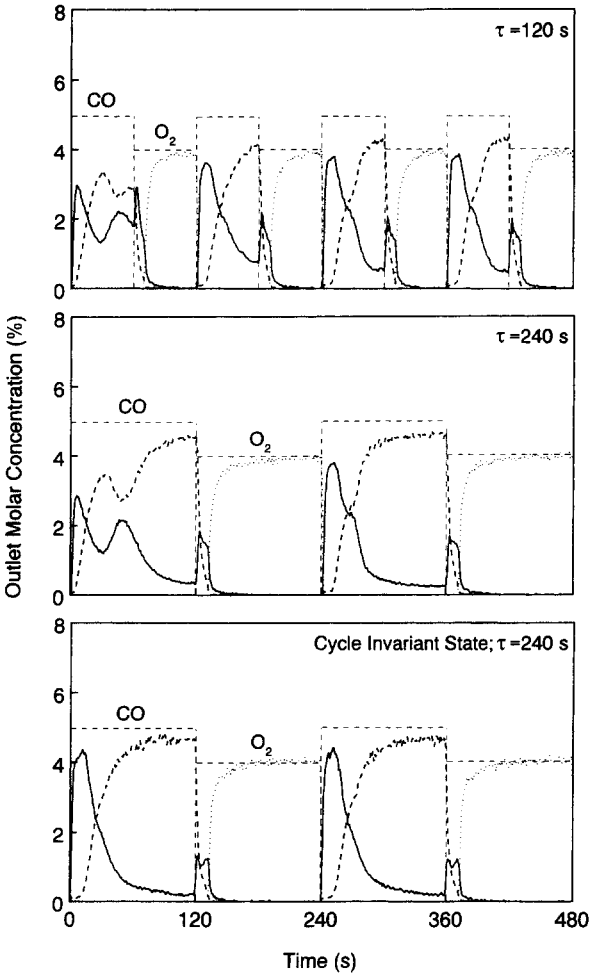

Fig. 3. Inlet and outlet concentration profiles of CO, O_2 and CO_2 after the start-up of oscillations at a period of 120 and 240 s as well as the cycle invariant state at a period of 240 s. (———), CO_2; (· · ·), O_2; (— — —), CO.

duced by oxygen on LH sites although the in-plane oxygen is almost depleted by reduction. This "new" oxygen in the second layer originates from the bulk by solid state diffusion. It has been reported recently [23] that even oxygen from the support can diffuse into the CuO phase in reasonable time scales. As is obvious from Fig. 3 for a period of 120 s this third stage reduction cannot clearly be observed in view of the fact that before the oxidation cycle is started still a reasonable amount of in-plane oxygen is present.

The second CO cycle shows a pattern different from the first. One maximum has disappeared and no longer a clear distinction can be made between ER and LH reaction. This arises from the fact that at the present temperature of 493 K full oxidation of surface copper is no longer possible [24]. This means that the surface predominantly contains Cu_2O. The amount of overlayer oxygen is decreased, more empty sites are initially available for CO to adsorb and consequently LH reaction proceeds sooner as compared to the first reduction cycle. The second maximum shifts and partly coincides with the first peak representing the ER production of CO_2. Hence only a shoulder remains visible. In summary, the reduction model [15] also adequately predicts the reduction during the forced oscillations in the CO cycles.

Differences between the two cycle periods are noticed during the oxidation cycle. In the first experiment (τ=120 s) the switch to oxygen is imposed just after the second maximum in the reduction cycle, when both a reasonable amount of adsorbed CO and in-plane oxygen are present. Upon admission of oxygen CO_2 is produced instantaneously. The little shoulder which is observed is an indication for a second oxidation route. In the second experiment (τ=240 s) the switch is implemented when the surface is almost totally occupied by CO and oxygen transport from the subsurface is the limiting factor for CO_2 production. The shape of the CO_2 production peak is similar in nature as in case of τ=120 s but the total amount of CO_2 is significantly reduced. This difference does not arise from the CO_2 still present in the reactor during the switch to oxygen, so called CO_2 flushing. This was validated by an experiment in which after reduction a step was performed to helium instead of O_2 which gave nearly abrupt decrease to zero of the CO_2 concentration without maximum and tailing. It is therefore interesting to focus on the amount of CO_2 produced after the switch to oxygen because relevant information about the oxidation can be derived from these data. In Table 1 the CO_2 produced per mol Cu on the catalyst in the oxidation cycle as well as the height of the CO_2 peak right after the switch are given for various experiments.

Clearly a maximum is obtained in the CO_2 production for intermediate cycle periods of 100–120 s. Obviously the species present on the catalyst after 50–60 s feeding of CO are important for the CO_2 production. We may also conclude that no net influence of the concentration of oxygen is observed on the

Table 1
Production of CO_2 and the height of the CO_2 peak during the first oxidation cycle

Period (s)	Concentration O_2 (%)	Production CO_2 (mol/mol_{Cu})	Height of peak (%)
60	4.0	0.053	2.5
100	4.0	0.062	2.8
100	6.1	0.069	4.0
120	4.0	0.070	2.9
240	4.0	0.058	1.9
240	6.1	0.056	3.0

total production of CO_2. However, when we look at the initial rates of production by comparing the height of the peaks right after the step, approximately first-order in O_2 concentration is observed.

Furthermore, in Fig. 3 the response after 25 cycles is shown for a period of 240 s. Since the response does not change significantly per period, the so-called cyclic steady state is reached at this point. In the reduction cycle only one large CO_2 peak is observed, whereas during the oxidation cycle clearly two CO_2 production stages can be distinguished.

From the above it can be concluded that the reoxidation of the copper catalyst proceeds in at least two steps. In addition we saw that part of the oxidation reaction is first-order in oxygen. To study the oxidation and investigate the source of oxygen and CO for CO_2 production during oxidation, labelling experiments are enlightening as will be illustrated in the next section.

The increasing time average production with frequency in Fig. 2 can mainly be ascribed to the relatively higher CO_2 production during the oxidation cycle. For short periods (τ<40 s) the CO_2 production level remains finite till the end of the oxidation cycle.

3.2. *Forced oscillations of CO and $^{18}O_2$ (Type II)*

The reoxidation of the catalyst was studied using labelled oxygen. Fig. 4 shows the concentration profiles in time at a period of 240 s. The first cycle is identical to the first cycle in the previous experiments since the same CO concentrations were used and preoxidation was carried out in unlabelled oxygen. In the first cycle with labelled oxygen large amounts of unlabelled CO_2 are produced which is somewhat

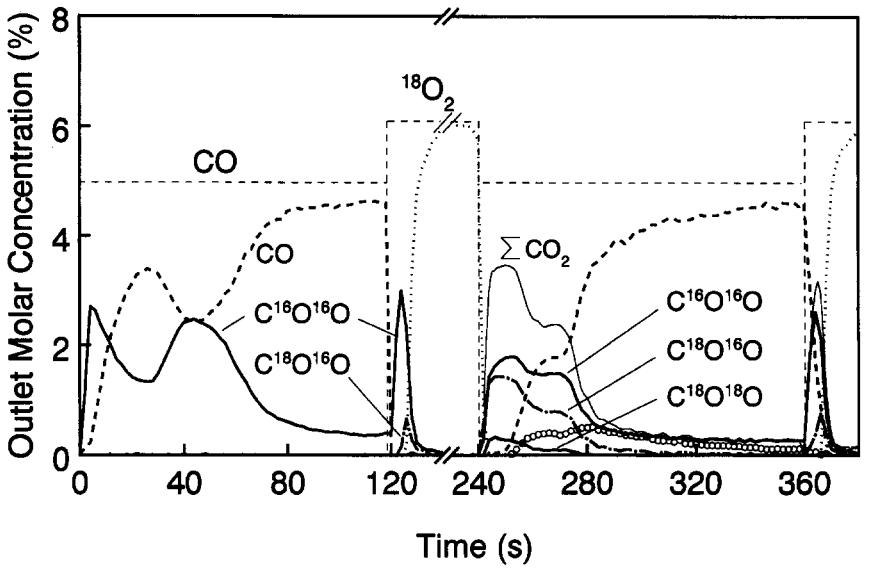

Fig. 4. Concentration profiles of labelled and unlabelled components after start-up of oscillations between CO and $^{18}O_2$ (τ=240 s). (○) $C^{18}O$. The catalyst is oxidised with $^{16}O_2$ at 773 K.

surprising. As before, no CO_2 was detected after a switch to He, so it can be concluded that both adsorbed $C^{16}O$ and ^{16}O are removed from the surface by $^{18}O_2$. In the long run we see in the oxidation cycle also some labelled CO_2 which is the shoulder observed in the type I experiments. Since this CO_2 is not instantaneously produced after the step to oxygen, a mechanism with consecutive reactions is assumed (see Section 3.4). Further O_2 does not seem to compete with CO for the same sites on the surface since no CO desorption is seen nor do we observe instantaneously produced labelled CO_2 upon a switch to $^{18}O_2$. A similar mechanism was proposed by Choi and Vannice [9].

The second reduction cycle provides insight in the exchange of oxygen during the reoxidation step. The fact that both $C^{16}O^{16}O$ and $C^{16}O^{18}O$ formed by an ER mechanism are observed indicates a rapid exchange between weakly bound overlayer oxygen and in-plane oxygen. However it must be noticed that the first peak of unlabelled CO_2 is not only due to ER mechanism since part of the CO_2 production may arise from LH reaction. Furthermore, the ratio CO_2 produced by ER over CO_2 produced via LH reaction calculated by taking peak height to be proportional to the amount produced by either ER or LH mechanism, is larger for single labelled than the same ratio for unlabelled CO_2. Nevertheless it is surprising how much of the originally present unlabelled oxygen still remains in the overlayer during the second reduction cycle.

The development of the production of labelled and unlabelled CO_2 during successive cycles for a cycle period of 100 s is presented in Fig. 5. A cycle invariant state is reached after 20 cycles at which point still a large amount of unlabelled CO_2 is observed. Subsurface oxygen cannot be the sole source of the ^{16}O. The total amount of ^{16}O released during 28 cycles exceeds the amount of oxygen originally present in the Cu phase on the catalyst (approximately 3.5 mole atomic ^{16}O is used per mole Cu). As also can be concluded from the formation of $C^{18}O^{18}O$ there is another source of ^{16}O. Moreover as shown in Fig. 6, $C^{18}O$ is observed within the reduction cycles which implies that ^{16}O is left on the surface. These observations prove the occurrence of dissociation of a CO bond on the Cu catalyst. Fig. 6 shows in addition that when the catalyst is reduced for a prolonged interval (τ=240 s), we noticed more net CO dissociation. It must be noted

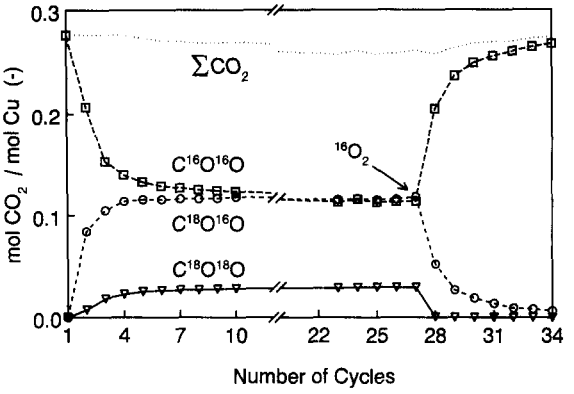

Fig. 5. Amount of labelled and unlabelled CO_2 produced per mole Cu during the reduction cycle versus the number of cycles (τ=100 s).

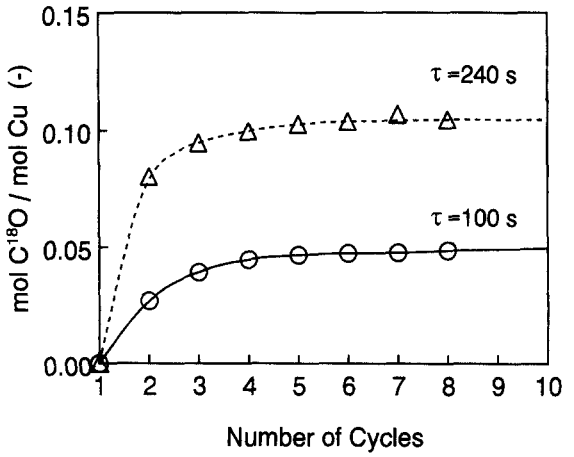

Fig. 6. Amount of $C^{18}O$ produced per mole Cu during the reduction cycle versus number of cycles for τ=100 s and τ=240 s.

that for both cycle periods the $C^{18}O$ concentration has dropped to zero well before a new cycle is started, so no direct influence of the cycle period is expected. The net dissociation does not cause any observable deactivation since the total CO_2 production was constant over at least 34 cycles (see Fig. 5). The fact that we did not observe any $C^{18}O$ or $C^{18}O^{18}O$ in the oxidation cycles implies once more that CO and O_2 adsorb non-competitively.

After 22 cycles at τ=100 s the mass balance of ^{16}O is as follows: 0.12 mol/mol$_{Cu}$ $C^{16}O^{16}O$ is produced

versus 0.025 and 0.050 mol/mol_{Cu} $C^{18}O$ and $C^{18}O^{18}O$, respectively. This leaves only 0.045 mol/mol_{Cu} ^{16}O which probably originates from the bulk or even from the support by a strong metal support interaction and solid state diffusion. In the long run this ^{16}O source will slowly be depleted.

Interestingly, the observed – effective – CO dissociation has never been observed for a Cu catalyst under the present conditions. A mechanistic explanation for this is found in methanol synthesis literature. Frost [25] and Millar et al. [26] noted that CO_2 is able to adsorb on a CuO or ZnO particle which contains defects by reduction. A metal–metaloxide combination forms a carboxylate species with CO_2 whereupon the carboxylate can decompose, thereby leaving oxygen on the surface. This mechanism would lead to a $C^{18}O$ production dependent on the concentration of $C^{18}O^{18}O$ and $C^{18}O^{16}O$ and the amount of defect, partly reduced sites. As the concentration of $C^{18}O^{18}O$ and $C^{18}O^{16}O$ is relatively high at the start of the second reduction cycle (see Fig. 4) and the amount of defect sites is high at the end of this cycle, the $C^{18}O$ concentration profile must contain an optimum approximately in the middle of the cycle, which is indeed the case (see Fig. 4; open circles). Furthermore a higher $C^{18}O$ production at longer reduction periods (Fig. 6; τ=240 s versus τ=100 s) can be explained as well by the fact that there will be more defect or reduced sites after longer reduction times.

Switching back to unlabelled oxygen (Fig. 5) results in a considerable amount of labelled CO_2 produced after one period, demonstrating that the catalyst acts as an oxygen buffer. Even at temperatures far below the pretreatment temperature of 773 K Cu can be oxidised in the oxidation cycle since we found labelled CO_2 for many periods after the switch to $^{16}O_2$.

In summary CO_2 production in the oxidation cycle proceeds in two stages. Instantaneous production of CO_2 in the oxidation cycle results from reaction of CO and O already adsorbed on the surface. In the second stage CO coordinated to Cu sites without in-plane oxygen reacts. To this end first oxygen has to adsorb on a vacant site nearest to this Cu site before reaction to CO_2 occurs. An illustrative representation of the mechanism is presented in Section 3.4. Furthermore the labelling experiments let us conclude that dissociation of CO effectively takes place, leaving oxygen on the surface of the catalyst during reduction. Adsorption of CO_2 on a partly reduced catalyst under formation of a carboxylate species and decomposition of this complex can be an explanation for the observed. In the next section we will focus on the structure of the active species and find support for the proposed mechanism using transient FTIR experiments.

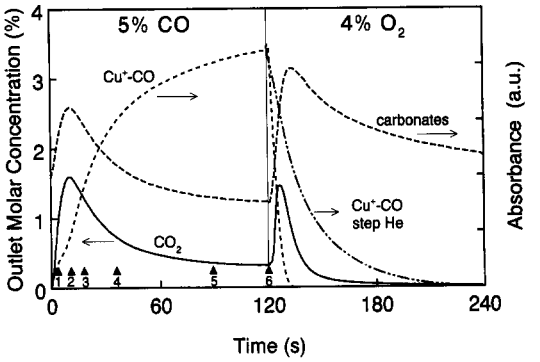

Fig. 7. Concentration of CO_2 and IR peak areas of carbonyl and carbonate groups in the cycle invariant state. Response on a switch to helium instead of oxygen is shown for the carbonyl group (– · –).

3.3. *Transient FTIR (Type III)*

In Fig. 7 the CO_2 concentration profile in the cycle invariant state is given as well as the areas of the IR peaks of the possible reaction intermediates: carbonyl (2000–2200 cm^{-1}) and carbonate-like (1200–1700 cm^{-1}) species. Whereas separate reduction by ER and LH mechanism were observed in type I experiments, we never saw two CO_2 production peak maxima in the IR experiments. Simulations show that this may be attributed due to the different reactor hydrodynamics of a fixed bed on the one hand and the FTIR cell on the other. The FTIR flow cell behaves approximately as a CSTR. In addition the catalyst may be changed by the preparation of the pellet.

Not clearly visible is the small amount of instantaneous formed CO_2 (Fig. 7), probably produced by ER mechanism. Subsequently a maximum is reached and the production slowly descends to a value which is approximately the same level as found in type I

experiments. Probably diffusion of oxygen from the subsurface determines the production at this point. The carbonyl band intensity increases rapidly with a small delay compared to CO_2. Within the reduction cycle the carbonyl band does not reach its maximum intensity. Whereas CO adsorption is very fast [17] the carbonyl band intensity increases only gradually. This suggests that CO–Cu^+ is an active reaction intermediate. Moreover the maximum in CO_2 production coincides with an inflection point in the carbonyl profile. So the reduction mechanism as proposed by us [15] properly describes the response in the sense that reduction proceeds in three steps.

The total carbonate absorbance (1200–1700 cm^{-1}) must be interpreted with care since the extinction coefficient of various types of carbonates differs significantly. More information is obtained by investigation of total spectra at various time scales discussed hereafter. The intensity of the carbonate band is correlated to the CO_2 concentration because presence of CO_2 always results in absorbance in the carbonate region [16]. However after the switch to oxygen the carbonates no longer follow the CO_2 response as delayed formation of these species is observed. The rather sharp maximum in CO_2 production, similar with observations in type I experiments, coincides with rapid decrease of carbonyl species. In order to verify that the steep decrease of carbonyl is not attributed to desorption of CO, in one experiment a step from 5% CO to helium was implemented (see the separate line in Fig. 7). In helium the decline of carbonyls is much slower, strongly suggesting that carbonyl and not the carbonate groups are the source of CO_2.

During oxidation the absorbance by carbonates remains more or less stable at a high level even in the absence of CO_2 and carbonyls. During successive reduction/oxidation cycles a steady increase in the carbonate occupancy is observed. Since a marginal influence on reactivity is found after dozens of cycles, the absolute amount of carbonates is likely to be small.

Additional information about the mechanism and surface species is obtained from Fig. 8, showing individual spectra at various time intervals during the reduction cycle. For all spectra the same background, the oxygen pretreated Cu catalyst, is taken. The CO_2 observed around 2350 cm^{-1} is gaseous CO_2.

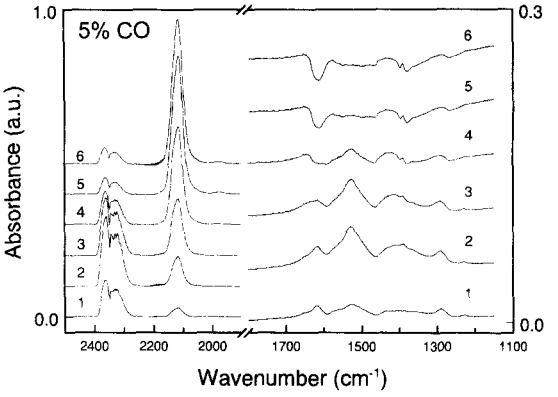

Fig. 8. Individual spectra during the reduction cycle. As background the fully oxidised catalyst at 493 K is taken. Numbers are denoted in Fig. 7.

Carbonyl species are observed at 2121 cm^{-1} upon introduction of CO in the cell. A shoulder at higher wave numbers, 2136 cm^{-1}, is developing while reaction proceeds. Both bands are due to carbonyl groups, whereas the low frequency band is often attributed to CO on Cu_2O [27]. The high frequency band cannot be assigned with certainty, though it has been reported that various oxidised Cu crystal faces give absorbance at wave numbers of 2115–2137 cm^{-1} [9]. Although the high frequency band increases during the CO cycle, the maximum of the carbonyl peak shifts from 2121 to 2116 cm^{-1} due to a net reduction of the surface of the catalyst. No CO on Cu^0 is observed as in that case we would expect a shoulder on the low frequency side of the 2121 cm^{-1} band, the region where CO–Cu^0 is expected [27]. However, we should take into account that the extinction coefficient for Cu^0–CO complexes is relatively low and absorption bands are probably hardly observed [28].

The various carbonate species are observed at 1200–1700 cm^{-1}. Table 2 gives an overview of assignments of carbonate complexes in a reducing but also in an oxidising environment [13,16]. The remaining intensity bands could not precisely be assigned to a carbonate complex. Monodentate and bidentate carbonate species have vanished after some time during the reduction while in oxygen when CO_2 already has disappeared still reasonable amounts are observed (not shown here), the bidentate carbonate band intensity even increases; both are relatively

Table 2
Assignment of IR bands in the 1200–1700 cm^{-1} region during CO oxidation on the Cu catalyst

Wave number (cm^{-1})	Species	Development in CO	Development in O_2
1640	Bidentate carbonate	Decrease	Increase
1585	Carboxylate (anti-symm.)	Minor increase	Decrease
1527	Monodentate carbonate	Present at high CO_2	Always present
1420	"Free" carbonate[a]	Following CO_2	Following CO_2
1392	Carboxylate (symm.)	Increase	Slight decrease

[a]Non-coordinated.

stable in an oxidising environment. Non-coordinated carbonates are following the CO_2 response closely and are also observed when CO_2 alone is introduced in the cell with the Cu catalyst. However, as mentioned before it is not very likely that the impact of the carbonates is significant and these groups are assumed to be spectators.

In view of the dissociation mechanism as proposed in Section 3.2 it is relevant to focus on the regions of absorption of the carboxylate group. During reduction of the catalyst an increase of absorbance due to the symmetrical as well as the anti-symmetrical stretching vibration is observed. This observation and the shift of the carbonyl group towards lower wave numbers due to a partial reduction of the catalyst, are both in agreement with the suggested mechanism. Therefore the dissociation of the CO bond is likely to occur via the carboxylate intermediate.

A remarkable negative absorbance at 1600 cm^{-1} compared to the oxidised catalyst could not be attributed to a surface specie. However we believe that a link between the removal of oxygen from the surface and this phenomenon is likely since the negative peak disappeared in oxygen. Possibly surface restructuring under reducing conditions, as for instance reported in [8], may cause this absorption. Metal oxygen fundamental vibrations are only found below 1200 cm^{-1} [13] and molecular oxygen (1500–1700 cm^{-1}) is not observed at high temperatures so these bands cannot be responsible for this observation.

3.4. Modelling of the reoxidation reaction

To verify the proposed mechanism for oxidation of the partly reduced catalyst and to determine the rate constants of the elementary steps, gas phase composition measured at the outlet of the reactor was fitted on several rate equations. Responses in the first oxygen cycle of experiments with periods of 60, 120 and 240 s were used. The objective function that was minimised by non-linear regression using a Simplex search routine for parameter estimation was:

$$\Phi = \sum_{i=1}^{n} (y^{obs}_{CO_2,i} - y^{calc}_{CO_2,i})^2 + \sum_{i=1}^{n} (y^{obs}_{O_2,i} - y^{calc}_{O_2,i})^2.$$

Modelling equations were solved by numerical integration (Runge–Kutta–Fehlberg algorithm) of partial differential equations using the Numerical Methods of Lines [29]. Axial dispersion is neglected since no differences were measured at the outlet between tracer experiments in an empty reactor and one filled with the Cu catalyst. In addition calculations showed that the axial dispersion coefficient is at maximum 10^{-4} m^2/s for the components of interest and no significant differences were obtained in simulations with and without axial dispersion using this coefficient. The partial differential equations were therefore of the following general form:

$$\frac{\partial c_j}{\partial t} = -v\frac{\partial c_j}{\partial z} + r_j\frac{1-\epsilon_b}{\epsilon_b} \quad (j \text{ denotes } CO_2 \text{ or } O_2),$$

$$\partial\frac{c_{k^*}}{\partial t} = r_{k^*} \quad (k^* \text{ denotes surface complexes}),$$

where v=0.11 m/s, ϵ_b=0.4 and the catalyst bed height was 0.010 m.

The mechanistic model for the reoxidation as derived especially from type I and II experiments, is depicted below. To illustrate the results as they were obtained in labelling experiments, the mechanism is written down as if it were a type II experiment: the oxygen used is isotopically labelled.

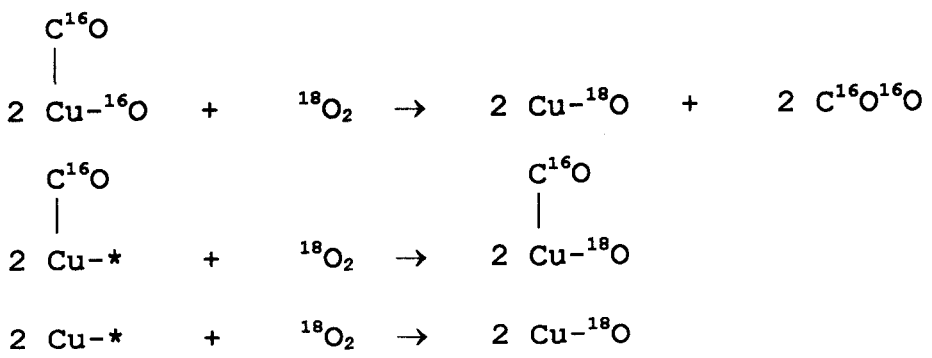

First oxidation takes place on sites where both CO and O are adsorbed and CO_2 is produced. Oxidation of sites on which only CO is present (2) leads to a new site which can react via step (1). In the labelling experiment this leads to the formation of a single labelled CO_2. Finally a third step is introduced because the amount of oxygen consumed in the oxidation cycle is much more than the amount of CO_2 produced. It is therefore obvious that besides sites containing CO other sites were oxidised as well without producing CO_2. The second reaction is assumed to be faster than reaction (3) because the product of the latter reaction cannot contribute to the oxidation in the second reaction step. More detailed presentation of the surface complexes is given in Fig. 10. The parameters to be determined are the initial fractions of COO*, CO* and * and values for k_1–k_3. The initial CO_2 concentration was measured at the outlet and assumed to be constant over the catalyst bed.

Attempts were made to fit all the parameters which did not result in accurate values for k_1 and k_2. Therefore reaction (1) and (2) were combined:

$$2COO\star + O_2 \rightarrow 2CO_2 + 2O\star \quad (1a)$$

$$2\star + O_2 \rightarrow 2O\star \quad (3)$$

In principle this would lead to erroneous results since CO* (2) is now also oxidised in one step and therefore half the amount of oxygen is needed for the oxidation of these species. However, the amount of oxygen consumed by this reaction is minor compared to the other steps as can be concluded from Fig. 4. The quantity of labelled CO_2 after the oxygen step is relatively small compared to the quantity of unlabelled CO_2. It will be shown that although not all kinetic constants could be estimated separately (k_{1a} is a lumped parameter) still valuable results are obtained concerning the reliability of this model, especially by focusing on the initial amounts of the surface species.

In the manner sketched, accurate values for all constants and initial values were obtained. In Fig. 9 the experimental values as well as the calculated concentrations are given for the three periods. Note that the experimental values for τ=120 and 240 s are the same as presented in Fig. 3; see the first 30 s of the oxidation cycles. We may conclude that the calculated CO_2 profiles approximate the observed ones closely. Although the measured O_2 development is not as well described as the CO_2 profile, the general trend is well predicted. Table 3 gives the estimated values of the

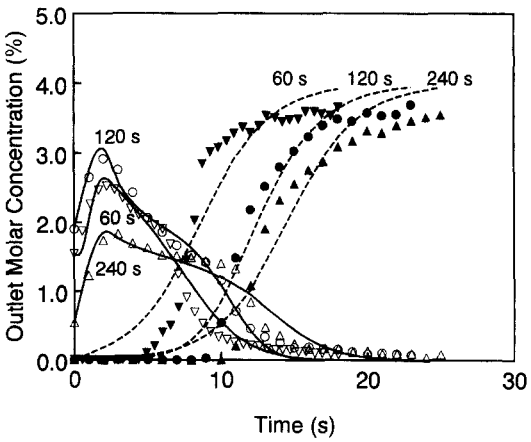

Fig. 9. Reoxidation of the catalyst in the first oxygen cycle for τ=60 s, τ=120 s and τ=240 s. Markers denote experimental values; lines denote the results obtained by mathematical modelling; CO_2: (———); O_2:(— — —).

Table 3
Estimated parameters for the reoxidation at various periods

Cycle period (s)	k_{1a} ($m^3\ mol^{-1}\ s^{-1}$)	k_3 ($m^3\ mol^{-1}\ s^{-1}$)	Initial $[CO_2^*]+[CO^*]$ (mol/mol_{Cu})	Initial [*] (mol/mol_{Cu})
60	0.65[a]	0.48±0.034	0.052±0.0023	0.13±0.021
120	0.65[a]	0.31±0.067	0.070±0.0083	0.21±0.030
240	0.65±0.016	0.35±0.029	0.058±0.010	0.27±0.053

[a]Parameter fixed at this value.

parameters and their 95% error intervals. k_{1a} was fixed at the value found for τ=240 s. No accurate value could be determined for small periods since the CO_2 concentration initially followed the input oxygen concentration for which a polynomial function was taken. This function was used to take into account the non-ideality of the concentration step.

The kinetic constants for the oxidation of sites resulting in CO_2 production were approximately twice as high as the constants of the oxidation of other sites. Nice agreement is observed between the initial amounts of CO containing sites and the amount of CO_2 produced according to Table 1. The estimated initial values can also be well explained by the knowledge we have about the mechanism. At a period of 60 s the switch to O_2 is made when only few sites are totally reduced so the amount of empty reduced sites is lowest of the three periods. Also a comparatively small amount of CO containing sites are present; the production by the LH reaction has not yet reached its maximum at the step to the oxygen cycle (see Fig. 3, t=30 s) and there are only a few sites on which CO can adsorb. In the 120 s experiment the switch was performed just after the maximum in LH reaction. Therefore many CO containing sites with adsorbed oxygen in the neighbourhood are present. Reduction has not proceeded to the extent as for τ=240 s, so the amount of reduced sites is in-between the values at τ=60 and τ=240 s. Finally we see comparatively more reduced sites at τ=240 s which is obvious since the reduction cycle is longer. Less CO containing sites are present than for τ=120 s since more CO has been converted by LH reaction and almost all the oxygen has reacted. Hence, the introduced oxygen reacts first with sites on which only CO is present whereupon in a second step CO_2 is produced. By that time part of the CO will have been desorbed and less CO_2 will be observed, as indeed is the case.

4. Conclusions

Vital information on the oxidation of CO over Cu-on-alumina could in an elegant manner be obtained by separately investigating the reduction/oxidation processes in successive reaction cycles. In agreement with earlier work the reduction of the fully oxidised catalyst was shown to proceed first by removal of overlayer oxygen via an ER mechanism (Fig. 10)(a) and subsequently by removal of in-plane oxygen via an LH mechanism (b). Concurrent to the latter, in-plane oxygen is slowly replenished by subsurface

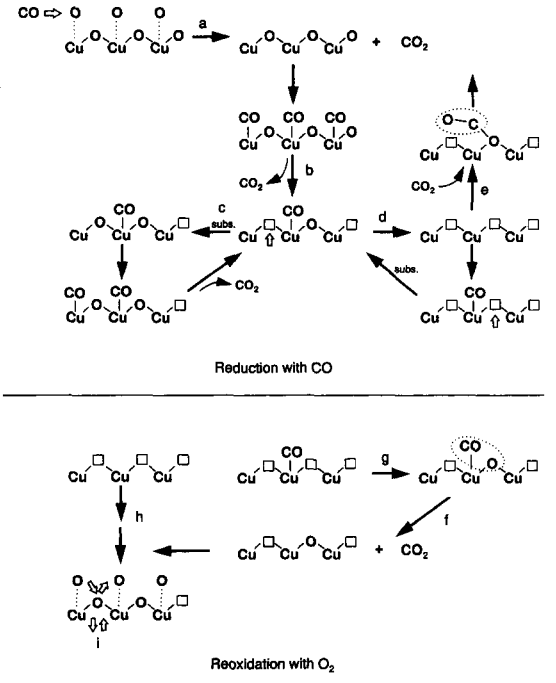

Fig. 10. Schematic representation of reduction with CO and reoxidation with O_2 of an alumina supported Cu catalyst at 493 K.

oxygen diffusion (c); or the catalyst can be further reduced (d). An intriguing phenomenon is the fact that during an extended period of subsequent reduction (with $C^{16}O$) and reoxidation (with $^{18}O_2$), the oxidation process is accompanied by the release of substantial amounts of $C^{16}O^{16}O$. The origin of the second ^{16}O can only be explained by an effective dissociation of CO, as is confirmed also by the observed $C^{18}O^{18}O$ and $C^{18}O$ production. This is all the more true for a severely reduced catalyst, containing relatively many defect sites. A mechanism in which CO_2 adsorbs on these sites under formation of carboxylates and subsequently decomposes towards CO and an oxidised species, is proposed (e).

For the reoxidation a mechanism is suggested incorporating three steps which can describe the response in the oxidation cycle satisfactorily. The first step (f) is oxidation of sites with adsorbed CO and O, and results in instantaneous production of CO_2. The second step (g) is oxidation of a site with adsorbed CO without in-plane oxygen present. Subsequently these oxidised species give CO_2 via (f). Finally also sites are oxidised without production of CO_2 (h). Exchange of in-plane oxygen with bulk oxides and with oxygen in the overlayer is shown for the reoxidised species (i). Note that in the present study only a mechanism is given for the reoxidation during the first reduction/oxidation cycles. As demonstrated in the labelling experiments after subsequent cycles a mechanism in which a net CO dissociation is incorporated as oxygen source, will be unavoidable. In future work we will focus on reoxidation and reduction mechanism after many successive reduction and oxidation cycles.

It was further demonstrated that the formation of CO_2 during the reoxidation cycle is accompanied by a rapid decrease in copper carbonyl, not attributable to desorption. Hence, the formation of CO_2 is likely to proceed over these carbonyl species rather than through other intermediates such as carbonates in accordance with the mechanism presented above. It is shown that apart from the carboxylate groups the carbonates probably are spectators without any contribution to the reactions of our interest.

The presented study is an example of the use of forced oscillations in heterogeneous catalysis. Mechanistic insights could be gained from experiments with transients at different time scales, oscillations at various periods.

5. Nomenclature

5.1. Symbols

c_i	Concentration of component i (mol/m^3)
d_i	Inside diameter of the reactor (m)
k_j	Reaction rate constant of reaction setp j (see text)
t	Time (s)
v	Gas velocity in the chamber (m/s)
V_1	Volume of the inlet chamber of the IR cell (m^3)
V_2	Volume of the outlet chamber of the IR cell (m^3)
y_i^{obs}	Observed fraction of component i at the reactor exit (-)
y_i^{calc}	Calculated fraction of component i at the reactor exit (-)
z	Axial distance along the catalyst bed (m)

5.2. Greek letters

ε_b	Void fraction of the catalyst bed (-)
τ	Cycle peroid (s)
Φ	Objective function to be minimised

References

[1] R.R. Sadhankar and D.T. Lynch, J. Catal., 149 (1995) 278.
[2] M.A. Mc Neil and R.G. Rinker, Chem. Eng. Commun., 127 (1994) 137.
[3] F. Qin and E.E. Wolf, Chem. Eng. Sci., 50 (1995) 117.
[4] J. Thullie and A. Renken, Chem. Eng. Sci., 48 (1993) 3921.
[5] M. Marwood, F. van Vyve, R. Doepper and A. Renken, Catal. Today, 20 (1994) 437.
[6] R.R. Sadhankar and D.T. Lynch, Chem. Eng. Sci., 51 (1996) 2061.
[7] J.S. Arlow and D.P. Woodruff, Surf. Sci., 180 (1987) 89.
[8] W.W. Crew and R.J. Madix, Surf. Sci., 349 (1996) 275.
[9] K.I. Choi and M.A. Vannice, J. Catal., 131 (1991) 22.
[10] J. Sanyi and D.W. Goodman, Catal. Lett., 21 (1993) 165.
[11] Y. Yao, J. Catal., 39 (1975) 104.
[12] R.A. Prokopowicz, P.L. Silveston, R.R. Hudgins and D.E. Irish, React. Kinet. Catal. Lett., 37 (1988) 63.
[13] A.A. Davydov, Infrared Spectroscopy of Adsorbed Species on the Surface of Transition Metal Oxides, Wiley, Chisester, UK, 1990 and references therein.
[14] G.K. Boreskov, Kinet. Katal., 11 (1970) 374.
[15] F.H.M. Dekker, G. Klopper, A. Bliek, F. Kapteijn and J.A. Moulijn, Chem. Eng. Sci., 49 (1994) 4375.

[16] J.W. Bijsterbosch, Copper based catalysts for CO oxidation and NO reduction, Ph.D. Thesis, University of Amsterdam, 1993.
[17] F.H.M. Dekker, M.C. Dekker, A. Bliek, F. Kapteijn and J.A. Moulijn, Catal. Today, 20 (1994) 409.
[18] H. Miura and R.D. Gonzalez, J. Phys. E.: Sci. Instrum., 15 (1982) 373.
[19] F.J.R. van Neer, D.S. Brands, B. van der Linden, A. Bliek, An IR Flow Cell for the Study of Transient Kinetics in Heterogeneous Catalysis, in preparation.
[20] J. van de Berg, A.J. van Dillen, J. van de Meijden, J.W. Geus, in: J.P. Bonelle et al. (Eds.), Surface Properties and Catalysis by Non-Metals, Reidel, Dordrecht, 1983, p. 493.
[21] T.J. Huang, T.C. Yu and S.H. Chang, Appl. Catal., 52 (1989) 157.
[22] F.J.R. van Neer, A.J. Kodde, H. den Uil and A. Bliek, Can. J. Chem. Eng., 74 (1996) 664.
[23] R. van Wijk, C.H.M. Marée, O.L.J. Gijzeman, F.H.P.M. Habraken and J.W. Geus, Appl. Surf. Sci., 99 (1996) 197.
[24] F.H.M. Dekker, Transient Kinetics in Heterogeneous Catalysis, Ph.D. Thesis, University of Amsterdam, 1995.
[25] J. Frost, Nature, 344 (1988) 577.
[26] G.J. Millar, C.H. Rochester, S. Bailey and K.C. Waugh, J. Chem. Soc. Faraday Trans., 89 (1993) 1109.
[27] G. Busca, J. Mol. Catal., 43 (1987) 225.
[28] M.L. Shepot'ko, A.A. Davydov and A.A. Budneva, Kinet. Catal., 35 (1994) 563.
[29] W.E. Schiesser, The Numerical Method of Lines: Integration of Partial Differential Equations, Academic Press, San Diego, CA, 1991.